

CORRELATING THE SEASONAL BEHAVIOR OF POLAR WARMING AND O₂ IR NIGHTGLOW

A. S. Brecht (amanda.s.brecht@nasa.gov), NASA Ames Research Center, Moffett Field, CA, USA, **L. Gkouvelis**, NASA Postdoctoral Program, NASA Ames Research Center, Moffett Field, CA, USA, **R. J. Wilson**, **C. E. Harman**, **M. A. Kahre**, NASA Ames Research Center, Moffett Field, CA, USA, **A. Kling**, Bay Area Environmental Research Institute, Moffett Field, CA, USA.

Introduction:

Mars' meridional circulation impacts the climate through the transport of heat, water, dust, and trace gases. The meridional circulation in the middle atmosphere is instrumental in the exchange of water between hemispheres and the expansion phase of large regional- and global-scale dust storms. The overall nature and structure of the mean meridional circulation (i.e., the Hadley cell) in the Martian atmosphere has been widely studied but the detailed behavior is still being investigated. To provide a more detailed examination of the meridional circulation, two features driven by the mean circulation will be analyzed as proxies. The first feature is polar warming (PW), which is dynamically induced due to the compressional heating of air in the descending branch of the Hadley cell. The second feature is O₂ IR nightglow emission in the 1.27 micron band, which is the result of a three-body recombination ($O+O+CO_2 \rightarrow O_2^*+CO_2$) and is largely dependent on the transport of dayside produced chemistry. By characterizing their seasonal sensitivities due to known lower atmosphere circulation drivers and correlating them, we will advance our knowledge of the meridional circulation.

Motivation:

Polar warming is characterized by a reversed (poleward) meridional temperature gradient in the middle-to-high latitudes all year, except local summer. It usually occurs between ~50 km and 80 km and ranges in magnitude from several to tens of Kelvin. It has been observed and discussed since the early 1970's (e.g., Conrath et al., 1973; Conrath et al., 1981; Martin and Kieffer, 1979; Jakosky and Martin, 1987; Deming et al., 1986; Smith et al., 2001; Keating et al., 2003; Tolson et al., 2007; Bougher et al., 2006; McCleese et al., 2007, 2008, 2010; Kleinbohl et al., 2009; McDunn et al., 2013; Forget et al., 2009). McDunn et al. (2013) provides the most quantitative set of parameters of observed PW based upon MRO/MCS-derived atmospheric temperatures. The study identifies PW trends that suggest that the structure of the mean meridional circulation is complex and not fully understood. Such trends are: (a) the southern hemisphere annual maximum PW occurs during late local winter of Martian year (MY) 29 and MY 30, (b) southern winter and northern winter solstices have similar PW magnitudes, and (c) the equinoctial seasons demon-

strated hemispheric asymmetry in PW magnitude (McDunn et al., 2013).

The O₂ IR nightglow emission is a product of 3-body reaction that occurs in areas of converging circulation. The nightglow becomes a valid tracer of circulation due to the chemical sources (atomic oxygen) largely produced on the dayside through photolysis (CO₂ and O₃). Chemical species (CO₂, O₃, O, etc.) are then transported by the circulation (day to night; equator to pole) to a region of favorable condition for recombination and subsequent de-excitation (i.e., emission). The O₂ IR nightglow emission at Mars produces a lower intensity compared to Venus and Earth, however it has been observed by orbital missions; Mex/OMEGA (Bertaux et al., 2012), Mex/SPICAM (Fedorova et al., 2012), and MRO/CRISM (Clancy et al., 2012, 2013). As with the PW, the nightglow is observed over high northern and southern latitudes between 40 – 60 km in altitude. The observational trends of the vertically integrated emission are: (1) the northern winter solstice has more intense emission than the southern winter solstice, and (2) the lowest peak altitude occurs during northern winter solstice. These trends seem to support the general concept of the role of the mean meridional circulation, unlike some of the PW trends (Clancy et al., 2012).

Past numerical modeling has been focused on either PW or the O₂ IR nightglow, but not both. In general, numerical models seem to under-predict the PW and over-predict the O₂ IR nightglow emission in comparison to observations (e.g., Haberle et al., 1982; Barnes and Haberle, 1996; Wilson, 1997; Forget et al., 1999; Clancy et al. 2012, 2013).

The observations are suggesting these two features, which are driven by the same circulation and are co-located, respond to the mean meridional circulation differently with respect to seasons. We will investigate the seasonal behavior of these features with respect to different atmospheric conditions and evaluate the trends.

Methods:

The current NASA Ames Mars Global Climate Model (MGCM), as described in Kahre et al., (this meeting), is utilized to characterize the seasonal response of PW and the O₂ IR nightglow emission to different dynamical drivers and their correlations simultaneously. Examining the drivers of PW and O₂ IR nightglow emission will provide a deeper

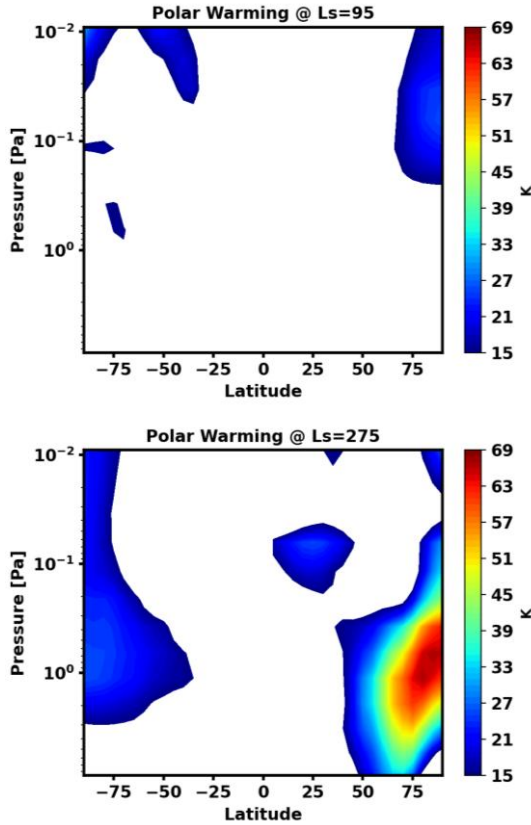


Figure 1: Polar warming for cloud case. Night time (22-2 LT), zonal average, binned $10^\circ L_s$, 5° Lat . understanding of the meridional circulation and how it impacts transport of other elements (e.g., water, dust). The work shown here uses a single MGCM set up. We

use a background dust scenario, which is constructed from the Montabone scenarios (MY29-34) by identifying the spatially and seasonally varying minimum value of the multi-year record to filter out the influence of episodic regional dust storms. For this specific application, the dust scenario is zonally averaged. The vertical dust distribution is governed by a latitudinally and seasonally varying prescription similar to Forget et al. (1999). The water ice clouds are radiatively active and solar flux is set for solar moderate conditions. Orographic and non-orographic gravity waves are not enabled for this simulation.

The simulated fields are binned in L_s (10°) and latitude (5°), zonally averaged, specifically looking at nightside (local time = 22-02).

The polar warming magnitude is quantified as described in McDunn et al., 2013:

$\Delta_p T(\text{Lat}) = [T_{\text{Lat}} - T_2]_p$; $\text{Lat}_{T_2} < \text{Lat} \leq T_1$, where T_1 is the largest bin-averaged temperatures in each hemisphere, T_2 is the smallest bin-averaged temperature between Lat_{T_1} and the equator, Lat_{T_1} is the latitude of T_1 and Lat_{T_2} is the latitude of T_2 . Following McDunn et al. (2013) temperature enhancement larger than 15 K is used to identify PW.

The O_2 IR nightglow volume emission rate (VER) is calculated using the following expression: $E(\text{O}_2^*) = (a \cdot k_1 \cdot [\text{O}] \cdot [\text{O}] \cdot [\text{CO}_2]) / (1 + t \cdot (k_{\text{CO}_2} \cdot [\text{CO}_2]))$ where a is the total yield of O_2^* , k_1 is the rate coefficient for the three-body recombination reaction, $[\text{O}]$ and $[\text{CO}_2]$ are concentrations for each specie, t is the lifetime by radiative relaxation of O_2^* , k_{CO_2} is the quenching coefficient for CO_2 . Current values for this simulation are: $a = 0.75$, $k_1 = 2.5 \cdot 5.2 \cdot 10^{-35} \cdot \exp(900/T) \text{ cm}^6 \text{ s}^{-1}$, $t = 3800 \text{ s}$, $k_{\text{CO}_2} = 2.0 \cdot 10^{-20} \text{ cm}^3 \text{ s}^{-1}$. Some of these values are not well known, so sensitivity tests will need to be conducted.

Preliminary Results:

Polar Warming. Figure 1 demonstrates the nightside polar warming calculated from the MGCM. For this simulation, $L_s = 90^\circ$ (Fig. 1 top) has minimal ($\sim 15 \text{ K}$ in northern hemisphere) to no PW. The MCS derived PW for $L_s = 90^\circ$ was less than 15 K during MY 29 in both hemispheres. However, MY 30 had a maximum of $\sim 30 \text{ K}$ in the southern hemisphere and $\sim 15\text{-}20 \text{ K}$ in the northern hemisphere (McDunn et al. 2013).

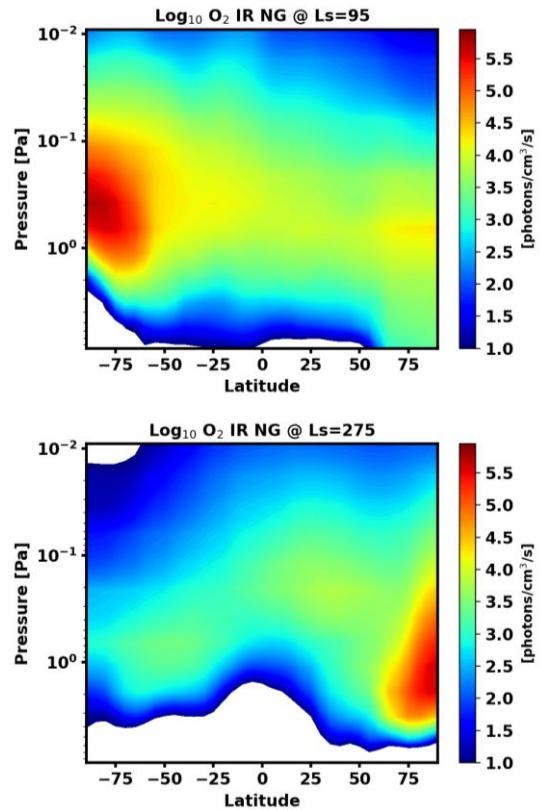


Figure 2: O_2 IR nightglow volume emission rate for cloud case. Night time (22-2 LT), zonal average, binned $10^\circ L_s$, 5° Lat .

The northern winter solstice ($L_s = 270^\circ$; Fig. 1 bottom) has PW magnitudes as large as 70 K in the northern hemisphere and $\sim 20 \text{ K}$ in the southern hemisphere. The MCS derived PW for $L_s = 270^\circ$ was largest overall in MY 28 with the maximum northern hemisphere $\sim 50 \text{ K}$ and southern hemisphere $\sim 30 \text{ K}$.

This Mars year also had a solstitial-season global dust storm. Both MY 29 and MY 30 resulted in northern hemisphere PW ~ 30 K and southern hemisphere PW ~ 15 K (McDunn et al., 2013).

This general trend of the simulated larger PW near northern winter solstice compared to southern winter solstice is consistent with the expected seasonal variation in the strength and extent of the mean meridional

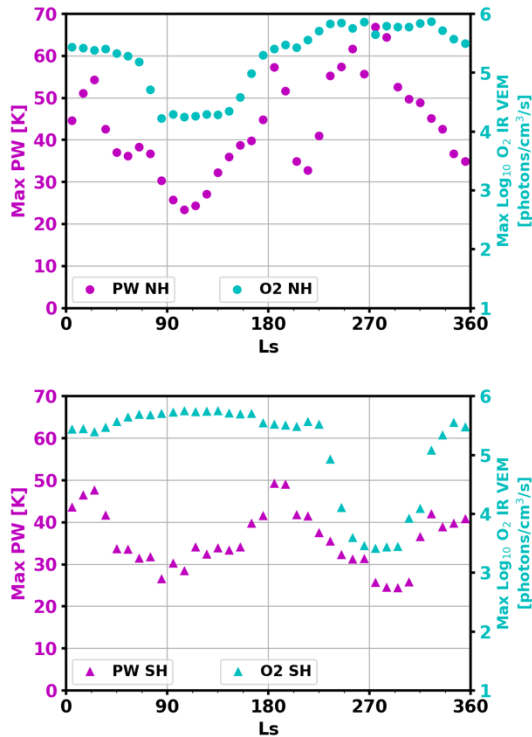


Figure 3: Maximum values of polar warming and log O_2 IR nightglow volume emission rate with respect to solar longitude (L_s). Night time (22-2 LT), zonal average, binned $10^\circ L_s$, 5° Lat. [Top] Northern hemisphere and [Bottom] Southern hemisphere.

circulation. However, the simulated behavior of the northern hemisphere PW at $L_s=90^\circ$ being larger than the southern hemisphere is not expected.

O_2 IR Nightglow Emission. Figure 2 demonstrates the simulated nightside O_2 IR nightglow VER. This simulation demonstrates the nightglow to be largest in the winter hemisphere with respect to solar longitude. The maximums are similar in magnitude for the southern winter solstice ($L_s=90^\circ$; Fig. 2, top) and northern winter solstice ($L_s=270^\circ$; Fig. 2, bottom) which would seem counter to what would be expected. The mean meridional circulation is observed to be stronger during $L_s = 270^\circ$, as the PW magnitudes in Figure 1 supports. Further examination and results will be compared to Clancy et al. 2012 and 2013, which discusses the MARCI CRISM O_2 IR nightglow emission observations.

Correlation. As discussed above, these features are driven by the same circulation and have been observed in similar spatial regions. Figure 3 shows

how the simulated maximum polar warming and O_2 IR VER vary seasonally; with the top panel representing the northern hemisphere and the bottom panel representing the southern hemisphere. In the north, the O_2 IR VER has a sinusoidal pattern, with a minimum near $L_s \sim 100^\circ$ and a maximum near $L_s \sim 270^\circ$. PW has a similar sinusoidal pattern but with an extra sizable decrease $L_s \sim 205^\circ$. The southern hemisphere shows the two features trending in opposite directions around $L_s = 90^\circ$ and then both trending toward a minimum near $L_s = \sim 290^\circ$. Clancy et al. (2012, 2013) presented the correlation between CRISM observed O_2 IR nightglow emission and MCS temperatures for $L_s = 74-137^\circ$, $Lat=70-90$ S, and altitude range of 50-60 km. They found the two features to be anticorrelated, as did the GCM results within that study. They claim, based on the southern hemisphere observations, that the correlation with adiabatic heating with O_2 IR nightglow emission is not very strong, but it seems to be largely dependent on the temperature dependent rate constant.

Future Work:

We will examine the behavior of the PW and O_2 IR nightglow VER and correlate their seasonal behaviors to provide more knowledge on the meridional circulation. We will extend the work of Clancy et al. (2012, 2013) by studying the full Martian year. The thermal and wind field, along with mass stream functions will also be reviewed. Moreover, several sensitivity cases will be conducted to investigate the relative importance of thermal (clouds and dust) and wave-induced forcing on the correlation between PW and O_2 IR nightglow VER, thus the meridional circulation.

References:

- Barnes and Haberle, *J. Atmos. Sci.*, 53, 1996; Bertaux et al., *J. Geophys. Res.*, 117, 2012; Bougher et al., *Planet. Space Sci.*, 54, 2006; Clancy et al., *J. Geophys. Res.*, 117, 2012; Clancy et al., *J. Geophys. Res.*, 118, 2013; Conrath et al., *J. Geophys. Res.*, 78, 1973; Conrath et al., *Icarus*, 24, 1981; Deming et al., *Icarus*, 66, 1986; Fedorova et al., *Icarus*, 219, 2012; Forget et al., *J. Geophys. Res.*, 104, 1999; Forget et al., *J. Geophys. Res.*, 114, 2009; Haberle et al., *Icarus*, 50, 1982; Jakosky and Martin, *Icarus*, 72, 1987; Keating et al., *Third International Mars Polar Science Conference*, 8033, 2003; Kleinbohl et al., *J. Geophys. Res.*, 114, 2009; Martin and Kieffer, *J. Geophys. Res.*, 84, 1979; McCleese et al., *J. Geophys. Res.*, 112, 2007; McCleese et al., *Nature Geoscience*, 1, 2008; McCleese et al., *J. Geophys. Res.*, 115, 2010; McDunn et al., *J. Geophys. Res. Planets*, 118, 2013; Smith et al., *J. Geophys. Res. Planets*, 106, 2001; Tolson et al., *J. Spacecraft and Rockets*, 44, 2007; Wilson, *Geophys. Res. Lett.*, 24, 1997